Polymer Testing 57 (2017) 235–244

Contents lists available at ScienceDirect

Polymer Testing

journal homepage: www.elsevier.com/locate/polytest

Material Properties

# Design of toughened PLA based material for application in structures subjected to severe loading conditions. Part 2. Quasi-static tensile tests and dynamic mechanical analysis at ambient and moderately high temperature

A. Bouzouita [a, b], D. Notta-Cuvier [a, *], R. Delille [a], F. Lauro [a], J.-M. Raquez [b], P. Dubois [b, c]

[a] LAMIH UMR CNRS/UVHC 8201, UVHC Le Mont Houy, 59313 Valenciennes Cedex 9, France
[b] LPCM, CIRMAP, University of Mons (UMONS), Place du Parc 20, B-7000 Mons, Belgium
[c] Department Materials Research and Technology, Luxembourg Institute of Science and Technology (LIST), Z.A.E. Robert Steichen,5 Rue Bommel, L-4940 Hautcharage, Luxembourg

ARTICLE INFO

*Article history:*
Received 14 October 2016
Accepted 24 November 2016
Available online 28 November 2016

*Keywords:*
Polylactide
Thermal properties
Toughening
Mechanical behavior under high temperature

ABSTRACT

The suitability of a ternary composition 58 wt% polylactide (PLA) - 25 wt% poly (methyl methacrylate) (PMMA) - 17 wt% Impact modifier (Biomax®Strong - BS) for use in technical parts subjected to severe loading conditions continues to be investigated. Previous work has demonstrated that PLA-PMMA-BS composition presents very appealing tensile properties at ambient temperature over a wide range of strain-rate, and can compete with petro-sourced blends for use in highly-loaded technical parts. Attention is paid now to its mechanical behavior at moderately high temperature (up to 60 °C), through tensile tests and dynamic mechanical analyses. Results highlight the improvement of mechanical properties in the considered range of temperature, thanks to the presence of PMMA in the blend, and prove that PLA-PMMA-BS composition can be suitable for use in technical parts subjected to high strain-rate and/or moderately high temperature.



## 1. Introduction

The demand for bio-based polymers, *i.e.* derived from renewable resources, is continuously growing in many industrial sectors, in particular because of the willingness to reduce the dependency on petro-sourced materials, to improve the recyclability of products and to answer customer expectations for materials with lower environmental footprint. Among currently available bio-based polymers, polylactide (PLA) is undoubtedly one of the most promising alternatives to petro-sourced polymers. First, PLA is biodegradable and may also offer recycling possibility at product end-of-life [1,2]. Above all, PLA has interesting mechanical properties, such as high flexural and tensile strength and rigidity, and can be processed using conventional equipment, in particular by injection molding [3]. Thanks to those interesting properties, PLA is now commonly used for some specific applications such as sustainable packaging. Recent breakthroughs allow the use of PLA for a wider range of applications (automotive components, electronic products, textile …) which require high performance materials [3–9].

Considering the particular case of the automotive industry, the use of polymers significantly increased over recent decades, thanks to appealing thermo-mechanical properties combined with low density and easy processing at high output rate and relatively low cost, generally by injection molding. Nowadays, many research projects aim to find sustainable alternative to conventional petro-sourced polymers. In that context, the use of PLA is undoubtedly appealing thanks to its high strength and rigidity, in particular. Therefore, PLA can already be found today in a few non-technical automotive interior parts, such as door trim [8], and its use should significantly increase in the future. Contrary to non-technical interior parts, automotive technical exterior parts can be subjected to severe loading conditions, in terms of high strain rate, combined with harsh conditions of temperature, humidity, etc. Hence, some properties of neat PLA are insufficient compared to those of traditional petro-sourced polymers like mineral-filled

* Corresponding author.
*E-mail address:* delphine.notta@univ-valenciennes.fr (D. Notta-Cuvier).

http://dx.doi.org/10.1016/j.polymertesting.2016.11.034
0142-9418/

polypropylene (PP) or acrylonytrile butadiene styrene (ABS)/polycarbonate (PC) blends for use in these parts. In particular, PLA is brittle, has low thermal and hydrolysis resistance, impact strength and crystallization rate [6]. However, PLA properties can be improved by combination with different additives: micro- and nano-fillers, impact modifiers, plasticizers, etc [4–6,10–12]. For instance, PLA nanocomposites with improved thermal stability and crystallization properties, together with preserved rigidity and stiffness, can be produced by combining PLA with various nano-fillers such as organo-modified layered silicates (OMLS), carbon nanotubes (CNT), graphite derivatives, polyhedraloligomeric silsesquioxanes (POSS), zinc oxide, etc [13–15]. Morerecently, quaternary compositions made of PLA, plasticizer (tributylcitrate - TBC), impact modifier (Biomax® Strong) and OMLS platelets (Cloisite® 25A) [4] or ternary compositions made of PLA, TBC and Halloysite nanotubes [5] were proven to be appealing alternatives to mineral-filled polypropylene for parts subjected to moderate loading rates at ambient temperature, with dramatically improved ductility and impact toughness together with satisfactory tensile strength and stiffness. However, the efficiency of plasticization to improve material ductility for durable applications is still an issue due to the possible migration of plasticizers over time [16],*e.g.*. In addition, plasticization has detrimental effect on heat resistance because it results in a decrease of glass transition temperature. For those reasons, the use of an impact modifier as an alternative to plasticizers in order to increase PLAductility can be a successful strategy, as demonstrated for instance by Bouzouita et al. [6] who used commercial impact modifier Biomax® Strong 120 (Dupont). The first advantage is that the use of impact modifier did not lead to a dramatic drop of stiffness or to a decrease of glass transition temperature, contrary to what is generally encountered after plasticization [4,5], and a significant increase in ductility level and impact toughness was found [4,13]. Secondly, it is expected that the use of an impact modifier instead of a conventional plasticizer may increase the durability of compositions by limiting the risk of leaching over time, even if no aging study was performed by Bouzouita et al. [6]. However, neither did it improve the thermal resistance of PLA-based materials. On the contrary, it has been proven that the addition of poly (methyl methacrylate) (PMMA) into PLA can significantly improved the thermal properties of PLA-PMMA blends, with excellent thermal stability, evaluated in terms of heat deflection temperature (HDT), together with high miscibility and good aging behavior [6,17–20]. In addition, high storage and Young's modulus can be maintained in PLA-PMMA blends [6,20]. However, PLA-PMMA blends were brittle, which is an obstacle for use in many technical applications.

Based on those results, Bouzouita et al. have developed ternary blends made of PLA-PMMA matrix in association with impact modifier Biomax® Strong120 (hereafter called BS) [6]. They have demonstrated that combining PLA-PMMA blend with BS led to a dramatic increase of the ductility and impact toughness of the material without altering the thermal properties of PLA/PMMA matrix. Comparison of mechanical and thermal properties of PLA-PMMA-BS composition to those of an ABS-PC blend, frequently used in automotive parts, revealed that this composition can be suitablefor use in technical applications.

Current work is continuation of developments initiated by Bouzouita et al. [6]dealing with the design of toughened PLA-PMMA blends for automotive applications and, more generally, for use in technical parts possibly subjected to high loading rate under a wide range of temperature (typically −40 °C to 80 °C in automotive sector). In previously published Part 1 of the present article [7], an important step toward industrialization of PLA-PMMA-BS composition was taken by demonstrating that the material can be processed on an “industrial scale” (by extrusion followed by injection molding on industrial devices and at production rate compatible with the requirements of the automotive sector), while keeping promising thermo-mechanical properties. It was also demonstrated that PLA-PMMA-BS composition presents mechanical properties that can compete with those of a petro-sourced ABS-PC blend, over a wide range of loading rates, from quasi-static to dynamic loadingconditions (up to 50 $s^{-1}$), at ambient temperature. In Part 2, mechanical behavior of PLA-PMMA-BS is now investigated under higher temperature. First, monotonic tensile tests were performed at quasi-static loading rate of 10 mm/min at 50 °C. This temperature was selected as sufficiently high to provide new knowledge on mechanical behavior of PLA-based compositions while being lower than the glass transition temperature, $T_g$, of the composition (about 60 °C [6]). Then, dynamic mechanical analysis (DMA) was performed for loading/unloading cycle frequency varying from 5 $10^{-2}$ to 30 Hz and temperature varying from 20 °C to 60 °C, *i.e.* very close to $T_g$. Joint analysis of effects of frequency and temperature variation highlights the “time-temperature equivalence” principle for mechanical behavior. Mechanical properties of PLA-PMMA-BS composition were compared to those of PLA-BS, in order to assess the effect of PMMA addition, and to those of ABS-PC, as a reference to evaluate the potential of developed composition for a use in technical parts subjected to moderately high temperature.

## 2. Materials and experiments

### 2.1. Materials

Commercial grade poly (L-lactide) 4032D, supplied by NatureWorks, and hereafter called PLA, was used as received. Its principal characteristics are number average molar mass, $M_n$, of 133,500 ± 5000 g/mol, polydispersity index (PDI) of 1.94 ± 0.06 (as determined by size-exclusion chromatography in chloroform at 35 °C, using polystyrene standards for column calibration) and D-isomer content of 1.4± 0.2%, as determined by the supplier. Intrinsic viscosity of PLA is given by the Mark-Houwink law with $[\eta] = KM_v^a$, where K = 0.0131 mL/g and a = 0.759, at 30 °C in chloroform, and $M_v$ is the viscosity-average molecular weight [21].

Poly (methyl methacrylate), hereafter called PMMA, was supplied by Evonik, under commercial name Plexiglas® 8N. Its principal characteristics are $M_n$ = 50,000 ± 2000 g/mol and PDI = 2.1 ± 0.1.

Biomax® Strong 120, hereafter called BS, was provided by Dupont. BS is a commercially available ethylene-acrylate impact modifier bearing epoxy moieties specifically designed for PLA.

Ultranox®626A (from GE Specialty Chemicals) was used as a stabilizer at a content of 0.3 wt% in all PLA-based blends.

A commercial polycarbonate-modified acrylonitrile butadiene styrene (hereafter called ABS-PC) was chosen as a reference material for the evaluation of PLA-PMMA-BS performance because of its high strength, rigidity and energy of deformation, even under high strain rate and temperature, which explains its frequent use in automotive applications. It can be noted that properties of ABS-PC actually constitute a very challenging goal, since they are higher than those of most petro-sourced polymers used in automotive sector (for instance, tensile strength and rigidity of a 20 wt% mineral-filled polypropylene are 1.5 and 2 times lower than those of ABS-PC at 1 mm/min [5]). However, ABS-PC and PLA are available at a similar cost on the market. In the present study, ABS-PC blend is Novodur® H801, designed by Styrosolution for automotive interior and exterior parts ($M_n$ = 32,900 ± 3000 g/mol and PDI = 3.4 ± 0.1).

### 2.2. Optimal composition PLA-PMMA-BS

As described before, PLA-PMMA-BS compositions are developed in order to improve PLA impact toughness and ductility (thanks to the addition of BS) and thermal resistance (thanks to blending with PMMA), without altering too much the inherent high rigidity and strength of PLA.

In a previous study [6], the composition 58 wt% PLA - 25 wt% PMMA - 17 wt% BS (designated as PLA70/PMMA30/BS in work by Bouzouita et al. [6]) was selected as the one presenting the best compromise between impact toughness, tensile strength and rigidity, on the one hand, and ductility and thermal properties (in terms of heat deflection temperature - HDT), on the other hand (Table 1). In particular, elongation at break and impact strength were significantly increased thanks to the addition of BS, while tensile strength and rigidity remained at a satisfactory level. In the following, this composition will simply be referred to as PLA-PMMA-BS. PLA-BS will refer to composition 83 wt% PLA - 17 wt% BS.

It can be noted that those tests of selection of the optimal composition were performed on material specimens prepared at "laboratory scale" (compounding using Brabender internal mixer 50EHT and injection using a DSM Mini Injection Molding apparatus [6]). Then, it has been verified that appealing mechanical properties of composition PLA-PMMA-BS were kept when that material was processed using industrial facilities (see next section) and subjected to tensile loading under high strain rate (up to macroscopic strain rate of 50 $s^{-1}$), at ambient temperature [7]. Macroscopic strain rate is defined as the ratio of displacement rate by the initial length (in tensile direction) of specimen's region of interest (ROI). Therefore, higher value can be attained locally in the ROI. Tensile tests were characterized by an excellent repeatability at all investigated displacement rates (from 1 mm/min to 1 m/s, which corresponds to macroscopic strain rate from 5.55 $10^{-4}$ $s^{-1}$ to 50 $s^{-1}$). Moreover, tensile tests demonstrated that PLA-PMMA-BS has mechanical properties that can compete with those of ABS-PCfor use in highly-loaded automotive technical parts (Fig. 1 and Table 2).

### 2.3. Processing at industrial scale

In the presentstudy, PLA-based compositions were processed using facilities and process parameters compatible with an industrial production. Process conditions were exactly the same as those described in previous work by Notta-Cuvier et al. [7] (briefly reminded hereafter). It is worth noting that tensile tests at ambient temperature, analyzed in Part 1 of this study [7], and present tests at higher temperature were, therefore, performed on materials processed in exactly the same conditions and from the same production batch.

The extrusion step of PLA-PMMA-BS and PLA-BS was performed on an industrial extrusion device (Leistritz ZSE twin-screw corotating extruder). All compounds were blended together at a feeding rate of 1.5 kg/h anda screw speed of 50 rpm. After extrusion, PLA-based materials werepelletized and conditioned in hermetically closed bags. Pellets ofextruded PLA-based compositions and of as-received ABS-PC were then conditioned for 24 h at 50 °C (uncontrolled ambient humidity). They were then injection molded into rectangular thin plates (dimensions of about 96 × 166 $mm^2$, thickness of 3 mm) using facilities of Reydel, an automotive supplier. During injection, meltand mold temperatures were respectively of 210 °C and40 °C forPLA-PMMA-BS, 210 °C and 45 °C for PLA-BS, and 250 °C and 80°Cfor ABS-PC (following the recommendation of the supplier).

Finally, specimens were cut by water jet on the injected plates, with a geometry that depends on test purpose (cf next sections).

**Table 1**
Results of preliminary characterization of PLA-PMMA-BS [6].

| | Neat PLA | PLA-PMMA-BS |
|---|---|---|
| Glass transition temperature, $T_g$ (°C)[a] | 61 | 62.8 |
| Crystallinity ratio, $\chi_C$ (%)[a] | 3 | 3 |
| HDT (under 0.45 MPa - °C) | 54 | 58 |
| Notched impact strength (kJ.$m^{-2}$) | 24 ± 0.1 | 44 ± 2.5 |
| Elastic modulus (GPa) | 3.2 ± 0.1 | 2.5 ± 0.1 |
| Tensile strength (MPa) | 68 ± 2 | 49 ± 3 |
| Elongation at break (%) | 2.8 ± 0.2 | 116 ± 4 |

Tensile tests were performed at a displacement rate of 1 mm $min^{-1}$.
[a] From second heating scan of DSC analysis.

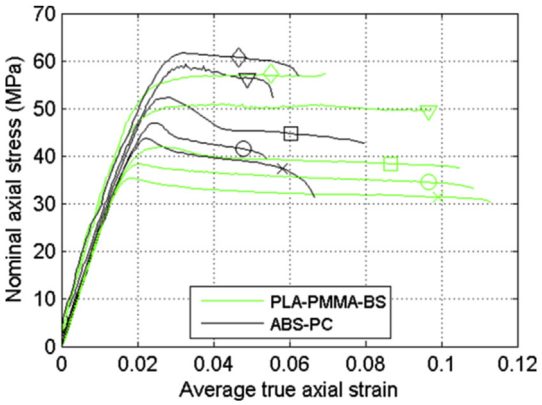


**Fig. 1.** Comparison of tensile behavior of PLA-PMMA-BS and commercial ABS-PC at different macroscopic strain-rate, $\dot{\varepsilon}$ (ambient temperature) [7] (x: $\dot{\varepsilon} = 5.55\ 10^{-4}\ s^{-1}$; ○: $\dot{\varepsilon} = 5.55\ 10^{-3}\ s^{-1}$; □: $\dot{\varepsilon} = 5.55\ 10^{-2}\ s^{-1}$; Δ: $\dot{\varepsilon} = 5\ s^{-1}$; ◊: $\dot{\varepsilon} = 50\ s^{-1}$).

### 2.4. Monotonic quasi-static tensile tests at 50 °C

Strain rate and temperature are known to significantly influence the mechanical behavior of polymers. After having studied strain rate sensitivity in Part 1, the present work now focuses on the analysis of the effect of temperature on the mechanical response of PLA-PMMA-BS composition, based on quasi-static monotonic tensile tests at 50 °C (*i.e.*approximately 10 °C below glass transition temperature ($T_g$)). To evaluate the benefits derived from the addition of PMMA, tests were also performed on PLA-BS blend. Mechanical behavior of PLA-based compositions was compared to that of ABS-PC. All the following information is common to tensile tests of all materials.

Quasi-static monotonic tensile tests were performed at displacement rate of 10 mm/min at 50 °C using an Instron E3000 electromagnetic tensile device (3 kN load cell sensor). As can be seen in Fig. 2, a climatic chamber was installed on the machine to allow testing at controlled temperature. Specimens were conditioned for 15 min in the oven before being gripped into the jaws. The temperature of the oven was imposed a few degrees higher (between 3 and 5 °C) than 50 °C so that the temperature on the specimen surface was 50 ± 2 °C (as checked using a non-contact IR thermometer before starting each test). The geometry of tensile specimen followed ISO527, with a cross-section of about 13 $mm^2$. The region of interest was 30 mm long, that corresponds to a macroscopic strain rate of 5.55 $10^{-3}$ $s^{-1}$. At least 5 tests were performed for each material.

During tensile tests, the nominal axial stress, σ, was computed by the ratio of the load applied to the specimen, F, (measured by load cell sensor at a frequency of 100 Hz) to the initial cross-section area of the specimen, $S_0$, so that $\sigma = F/S_0$. True in-plane strains were

**Table 2**
Tensile properties of PLA-PMMA-BS, PLA-BS and commercial ABS-PC at different displacement rates under ambient temperature (mean ± standard deviation for 5 tests per material and per displacement rate) [7].

| | Displacement rate | PLA-PMMA-BS | PLA-BS | ABS/PC |
|---|---|---|---|---|
| Elastic modulus (GPa) | 1 mm/min | 2.46 ± 0.02 | 2.10 ± 0.05 | 2.43 ± 0.01 |
| | 10 mm/min | 2.46 ± 0.03 | 2.17 ± 0.02 | 2.45 ± 0.02 |
| | 100 mm/min | 2.51 ± 0.07 | 2.13 ± 0.03 | 2.47 ± 0.05 |
| | 100 mm/s | 2.76 ± 0.07 | 2.48 ± 0.03 | 2.55 ± 0.04 |
| | 1 m/s | 2.91 ± 0.13 | 2.62 ± 0.24 | 2.81 ± 0.13 |
| Tensile strength (MPa) | 1 mm/min | 35.4 ± 0.3 | 26.0 ± 0.1 | 43.4 ± 0.4 |
| | 10 mm/min | 38.0 ± 0.4 | 28.8 ± 0.1 | 47.1 ± 0.4 |
| | 100 mm/min | 42.3 ± 0.6 | 33.4 ± 0.3 | 52.2 ± 0.1 |
| | 100 mm/s | 50.6 ± 0.4 | 43.6 ± 0.5 | 59.5 ± 0.4 |
| | 1 m/s | 56.9 ± 0.9 | 49.4 ± 0.6 | 62.3 ± 0.2 |
| Strain at break[a] | 1 mm/min | 0.116 ± 0.011 | 0.072 ± 0.018 | 0.058 ± 0.013 |
| | 10 mm/min | 0.109 ± 0.017 | 0.129 ± 0.015 | 0.052 ± 0.002 |
| | 100 mm/min | 0.104 ± 0.023 | 0.154 ± 0.018 | 0.086 ± 0.026 |
| | 100 mm/s | 0.080 ± 0.021 | 0.166 ± 0.019 | 0.055 ± 0.003 |
| | 1 m/s | 0.067 ± 0.007 | 0.112 ± 0.030 | 0.054 ± 0.017 |

[a] The given value of strain at break is the average of the axial strains computed by DIC in all facets of specimen ROI at specimen failure. For definition of facets, see section 2.4 or [7].

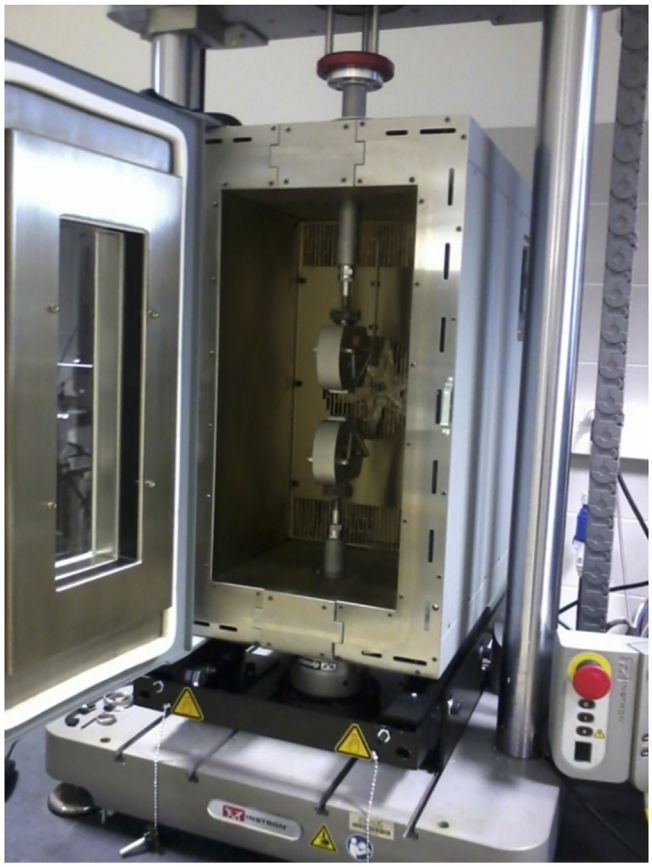

**Fig. 2.** Instron E3000 electromagnetic device and climatic chamber.

computed using displacement field measurements by digital image correlation (DIC) [7,22], using VIC2D software. True strains were computed over facets of 15 × 15 pix$^2$with a step size (distance between two consecutive points of measurement) equal to 7 pixels. It can be noted that 7 pixels corresponded to about 470 μm for the present experiments. For more details about the principle of DIC and selection of facet and step size the reader can refer to references [22] and [7], respectively.

In order to compute the elastic modulus, linear regression wasapplied to the initial linear part of the behavior curve, *i.e.* nominalaxial stress vs. average axial strain, for values of average axial strainvarying from 0 to 1%. The average axial strain is the average of trueaxial strain computed in all the facets of specimen ROI. It can benoted that the true axial strain remained homogeneous over thewhole specimen ROI (*i.e.*very similar values in all facets) at least up to3%, for all materials (*nota*: axial strainremained homogeneous over the ROI up to about 1% during tests performed at room temperature [7]). Therefore, theelastic modulus that is calculated with the average axial strain is anaccurate evaluation of the actual Young's modulus of the material.

It can be noted that quasi-static tests previously performed at room temperature ([7] and Fig. 1 and Table 2 in section 2.2) were performed on the same tensile device (same load cell and frequency of load acquisition but without the climatic chamber), using the same specimen geometry and DIC for strain measurement (same facet and step sizes and camera frame rate).

### 2.5. Dynamic mechanical analysis from ambient temperature to 60 °C

Dynamic Mechanical Analysis (DMA) was performed in order to investigate the viscoelastic behavior of PLA-based composition at ambient temperature and up to 60 °C (test temperature remained constant at a fixed value during each DMA, contrary to DMTA). The highest temperature was fixed at 60 °C, *i.e.* very close to $T_g$ (about 62 °C), in order to investigate the mechanical behavior of PLA-PMMA-BS at the vicinity of glass transition and to assess the validity of the "time-temperature equivalence" principle. DMA was performed using the same electromagnetic device as monotonic tensile tests, namely Instron E3000. Specimens were coupons of 50 × 10 mm$^2$ (thickness of about 3 mm). They were subjected to loading/unloading cycles at a frequency varying from 0.01 to 30 Hz (Table 3), at different temperature (room temperature, *i.e.* about 20 °C, 40 °C, 50 °C and 60 °C). Temperature on the specimen surface was checked using a non-contact IR thermometer before each testing. 2 tests per material and per temperature were performed, except at room temperature (3 tests).

During post-treatment, only cycles for which the maximum force was stabilized were kept for the computation of the storage modulus (E′), the loss modulus (E″) and the loss factor (tan δ). For each selected cycle, the storage modulus, E′, and the loss modulus, E″, were computed using the relationships $E' = \sigma_0/\varepsilon_0 \cos(\delta)$ and $E'' = \sigma_0/\varepsilon_0 \sin(\delta)$, respectively, where $\sigma_0$ is the amplitude of the sinusoidal axial stress resulting from the sinusoidal applied force, F

**Table 3**
Description of DMA protocol (common to all test temperature).

| Phase of DMA protocol | Number of imposed loading/unloading cycles and corresponding frequency |
|---|---|
| Phase 1 | 3 cycles at $10^{-2}$ Hz |
| Phase 2 | 3 cycles at 5 $10^{-2}$ Hz |
| | 4 cycles at 0.1 Hz |
| | 5 cycles at 0.25 Hz |
| | 7 cycles at 0.5 Hz |
| | 20 cycles at 1 Hz |
| Phase 3 | 100 cycles at 10 Hz |
| | 300 cycles at 20 Hz |
| | 500 cycles at 30 Hz |

($\sigma = F/S_0$ where $S_0$ is the initial cross-section of the coupon), and $\varepsilon_0$ is the amplitude of the sinusoidal axial strain. During DMA, the axial strain was computed by the ratio of the displacement of the movable jaw by the initial distance between the jaws. Last, $\delta$ is the phase lag between stress and strain. It can be noted that it is generally considered that the storage modulus measures the stored energy that represents the purely elastic behavior of the material, while the loss modulus measures the dissipated energy, hence representing the viscous part of behavior.

## 3. Results and discussion

### 3.1. Monotonic quasi-static tensile tests at 50 °C

Figs. 3 and 4 show the tensile behavior of compositions PLA-PMMA-BS, PLA-BS and ABS-PC when tested at a displacement rate of 10 mm/min and at a temperature of 50 °C (in Fig. 4, the envelop of behavior evolution is plotted with lower and upper bounds). All specimens of PLA-PMMA-BS and PLA-BS remained unbroken up to a jaw displacement of 55 mm (*i.e.* engineering strain higher than 1.83). The maximal strain that can be seen in Figs. 3 and 4 for those materials is, therefore, the maximal strain that is attainable at the maximal jaw stroke and not the strain at break. Hence, when tested at 50 °C, PLA-based compositions showed very high levels of ductility. However, contrary to the very good repeatability observed during quasi-static and dynamic tensile tests at ambient temperature [7], a noticeable variation of the stress-strain curves, with scattered values of rigidity and yield stress (Table 4), was observed for the present tests at 50 °C for PLA-PMMA-BS and PLA-BS. In contrast, tensile behavior at 50 °C of petro-sourced ABS-PC blend showed low dispersion.

Fig. 5 and Table 4 allow comparing mechanical behavior of materials at ambient temperature and at 50 °C. As expected, tensile properties of ABS-PC were slightly affected by the increase of test temperature, thanks to high thermal properties (glass transition temperature of about 125 °C and HDT A and B of 99 °C and 106 °C according to supplier's technical data sheet). Thus, elastic modulus and tensile strengthwere only divided by a factor 1.19 and 1.2, respectively, between tests at ambient temperature and 50 °C. In contrast, properties of PLA-based compositions were significantly affected by the increase of test temperature. Thus, average values of elastic modulus and yield stress of PLA-BS were respectively divided by 3.8 and 3.6. Thanks to the presence of PMMA, these ratios were lower for PLA-PMMA-BS (1.9 for both elastic modulus and yield stress based on average values).

These drops in elastic modulus and tensile stress were directly related to the proximity between glass transition temperature, $T_g$, of PLA-based compositions (respectively 61.6 °C and 62.8 °C for PLA-BS and PLA-PMMA-BS following our DSC analyses [6]) and test temperature. Indeed, the evolution of tensile behavior was characteristic of a transition to rubber behavior with drop in rigidity and strength and spectacular increase of elongation at break. However, it is notable that the addition of PMMA was undoubtedly beneficial for behavior of PLA-PMMA-BS, compared to PLA-BS (Fig. 5), even if the gain in $T_g$ was quite low (1.2 °C). Indeed, PLA-PMMA-BS showed satisfactory properties at 50 °C, with rigidity and strength of same order of magnitude of those of a mineral-filled polypropylene [5], for instance, and very high volume energy of deformation, at least of 29.6 mJ/mm$^3$ (minimum attainable value because this figure was computed based on behavior curve of unbroken specimens), to be compared to an average value of about 3 mJ/mm$^3$ for ABS-PC. On the contrary, properties of PLA-BS tested at 50 °C were prohibitive for use in technical parts.

To explain the scattering of tensile properties of PLA-based compositions at 50 °C, additional DSC analysis were performed on samples presenting the highest and weakest properties (*i.e.* PLA-PMMA-BS #5 and #4 and PLA-BS #4 and #2, respectively), using DSC Q2000 from TA Instruments at both heating and cooling rates of 10 °C/min under nitrogen. The glass transition temperature, $T_g$, enthalpy of cold-crystallization ($\Delta H_{cc}$), and.

melting enthalpy ($\Delta H_m$) were evaluated from the resulting DSC thermograms at the second heating scan. Crystallinity index of PLA ($X_c$) was determined using $X_c\,(\%) = (\Delta H_m\text{-}\Delta H_{cc})/(w_{PLA}.\,\Delta H_m^0)\times 100$, where $w_{PLA}$ is the weight fraction of PLA in the sample (53% here) and $\Delta H_m^0$ is the melting enthalpy for 100% crystalline PLA (93 J/g). Results presented in Table 5 shows that samples that exhibited the highest tensile properties at 50 °C were those with higher crystallinity ratio and Tg, and *vice versa.* Scattering of mechanical behavior at 50 °C can, therefore, be explained by a slight variation of $T_g$ and crystallinity of samples, which has an amplified impact when tests are performed at a temperature close to $T_g$.

### 3.2. Dynamic mechanical analysis from ambient temperature to 60 °C

Fig. 6 shows the DMA results for PLA-PMMA-BS composition, in terms of storage and loss modulus and loss factor, tan $\delta$. High-frequency (10, 20 and 30 Hz) cyclic tests at 60 °C were not useable because the load amplitude of cycles never stabilized. As expected, dynamic properties were sensitive to test frequency, due to viscoelastic behavior of the material. A major consequence of viscoelasticity is that the elastic modulus of a material subjected to a constant stress will decrease over time (with duration depending on considered material), because of molecular rearrangement in an attempt to minimized internal stress. Then, storage moduli computed over a short period (*i.e.* during a test at high frequency) are higher than those computed over a longer period (*i.e.* during a test at lower frequency). This trend was observed for PLA-PMMA-BS under all test temperatures (Fig. 6(a)). Storage modulus also depended on test temperature with value decreasing with temperature. Up to 50 °C, value of storage modulus remained satisfactory but a significant drop was noticed at 60 °C, especially for the

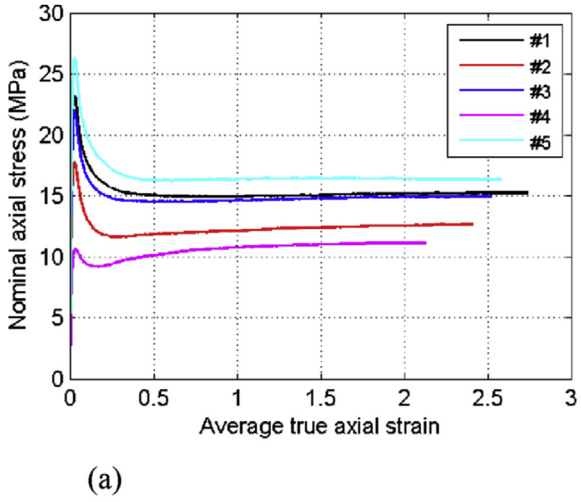


(a)

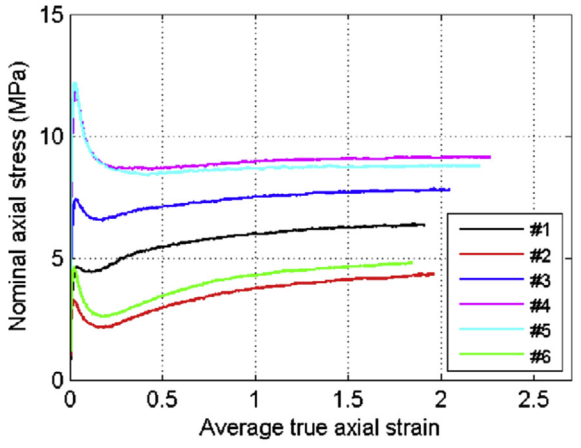


(b)

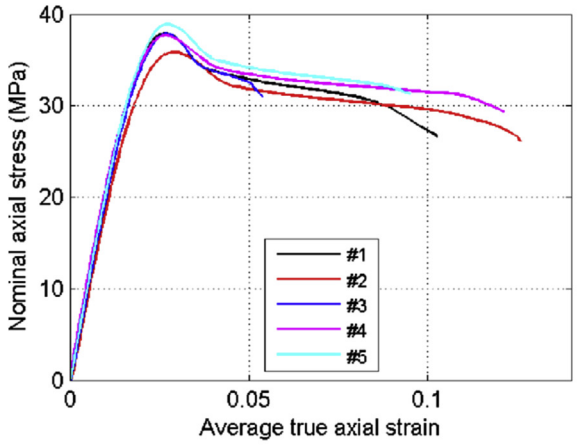


(c)

**Fig. 3.** Tensile behavior of (a) PLA-PMMA-BS (b) PLA-BS and (c) ABS-PC - 10 mm/min, 50 °C.

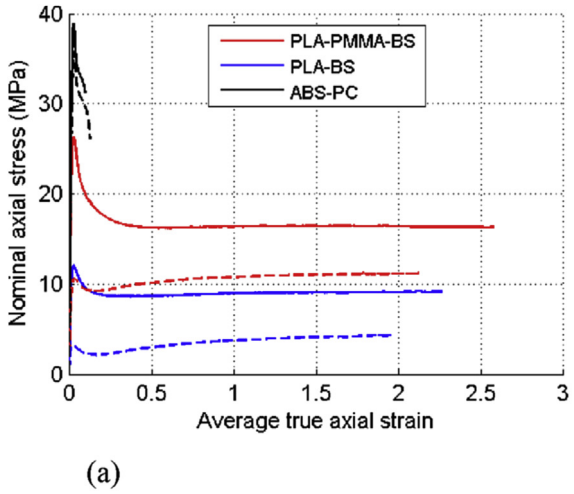


(a)

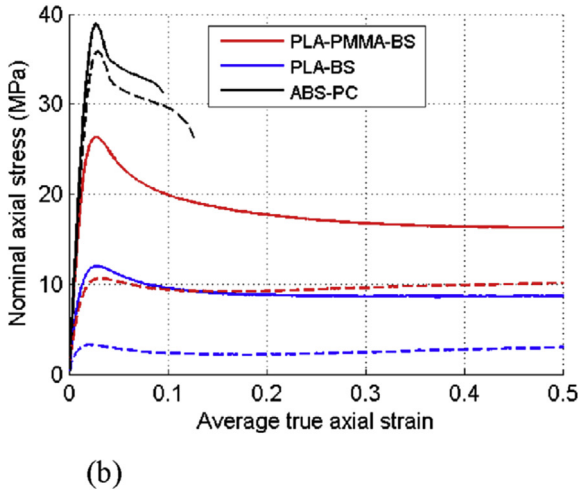


(b)

**Fig. 4.** Comparison of tensile behavior of PLA-PMMA-BS, PLA-BS and ABS-PC at 10 mm/min and 50 °C (continuous lines: upper bounds of behavior curves; dashed lines: lower bounds).(a) All data. (b) Focus on lower strain level

lowest frequency with rubber-like behavior. This is explained by the proximity between test temperature and glass transition temperature of the composition (62.8 °C [6]). It is interesting to note that results perfectly illustrate the "time-temperature equivalence" principle according to which decreasing strain rate (*i.e.* decreasing cycle frequency in case of DMA) is equivalent to increase test temperature. Thus, at the lowest frequency, the threshold of glass transition was fully crossed, leading to rubbery behavior of amorphous phase, while at higher frequency this threshold was very close but maybe not crossed, leading to a more "glassy" (*i.e.* rigid) behavior.

Contrary to storage modulus, loss modulus decreased when increasing frequency (except at 60 °C) and increased with temperature (except for the lowest frequencies at 60 °C), indicating that viscous behavior is more significant at low frequency (*i.e.* high period of time) and high temperature (Fig. 6(b)). As mentioned before, the evolution of loss modulus at 60 °C is markedly different than at lower temperature. It seems that the loss modulus reached a peak at about 1 Hz at 60 °C, thus indicating the proximity of the glass transition, which is characterized by nature by a maximum of

**Table 4**
Tensile properties of PLA-PMMA-BS, PLA-BS and ABS-PC at 10 mm/min, ambient temperature [7] and 50 °C (mean ± standard deviation).

| | Temperature | PLA-PMMA-BS | PLA-BS | ABS/PC |
|---|---|---|---|---|
| Elastic modulus (GPa) | Ambient | 2.46 ± 0.03 | 2.17 ± 0.02 | 2.45 ± 0.02 |
| | 50 °C | 1.32 ± 0.38 | 0.57 ± 0.27 | 2.06 ± 0.05 |
| Maximal stress (MPa) | Ambient | 38.0 ± 0.4 | 28.8 ± 0.1 | 47.1 ± 0.4 |
| | 50 °C | 20.1 ± 5.8 | 7.97 ± 3.5 | 37.8 ± 1.1 |
| Strain at break[a] | Ambient | 0.109 ± 0.017 | 0.129 ± 0.015 | 0.052 ± 0.002 |
| | 50 °C | Unconcerned | Unconcerned | 0.010 ± 0.029 |
| Volume energy of deformation (mJ/mm$^3$)[b] | Ambient | 3.61 ± 0.59 | 3.38 ± 0.40 | 1.85 ± 0.09 |
| | 50 °C | >29.6[c] | >12.3[c] | 2.99 ± 0.87 |

[a] Average of the true axial strains computed by DIC in all facets of specimen ROI at specimen failure.
[b] Volume energy of deformation, e, is defined by $e = \int_{\varepsilon=0}^{\varepsilon_{max}} \sigma d\varepsilon$ where σ is the nominal axial strain, ε the average true axial strain and $\varepsilon_{max}$ the average true axial strain at break or at the end of test in case of unbroken specimens.
[c] Minimum value attainable because e is computed on unbroken specimens. Given value is the average of all tests.

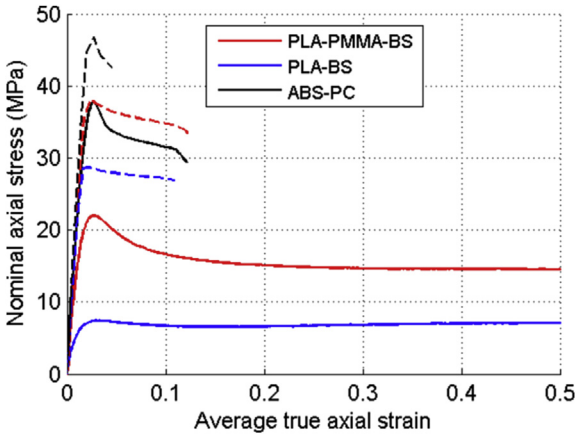


**Fig. 5.** Comparison of tensile behavior of PLA-based compositions and ABS-PC at ambient temperature (dashed lines) and 50 °C (continuous lines) - 10 mm/min. (Ambient temperature: tests arbitrarily chosen (behavior showed no dispersion [7]); 50 °C: samples PLA-PMMA-BS #3 and PLA-BS #3 (closest properties to average properties), sample ABS-PC #4).

dissipation phenomena, i.e. by a maximum of loss modulus [23]. However, crossing of glass transition temperature can also be evidenced by a peak of tan (δ). At 60 °C, this one was located at lower frequency (about $10^{-2}$ Hz - Fig. 6(c)) than peak of loss modulus. Actually, it is commonly observed that peak of tan (δ) is shifted to higher temperature, at fixed frequency, than peak of loss modulus [23,24]. According to "time-temperature equivalence" principle, it is equivalent to a shift to lower frequency at fixed temperature, as observed here. This principle was also illustrated by a decrease of tan (δ) when increasing load frequency, because the increase of loading rate moved the material away from transition to rubber behavior.

Fig. 7 (average over all tests) allows comparing the storage modulus of PLA-PMMA-BS and PLA-BS compositions. At all investigated temperatures and frequencies, the presence of PMMA had positive effect on storage modulus. At 50 °C, the storage modulus of PLA-PMMA-BS was higher than that of PLA-BS of about 200 MPa, whatever the test frequency. It is very interesting to note that, at 50 °C, the storage modulus of PLA-PMMA-BS was always higher than 1 GPa (except for two tests at $10^{-2}$ Hz with storage modulus of about 950 MPa). In contrast, storage modulus of PLA-BS remained lower than 1 GPa at 50 °C except for the highest test frequencies (the number of cycles at 10 Hz was not sufficient to attain the stabilization of load amplitude, which explains the absence of data at 10 Hz). At 60 °C, storage modulus of PLA-PMMA-BS dropped to values too low to allow its consideration for use in technical parts (lower than 600 MPa), and PLA-PMMA-BS presented rubber-like behavior at $10^{-2}$ Hz. However, its dynamic properties were undoubtedly better than those of PLA-BS that presented rubber behavior up to 1 Hz at 60 °C. In addition, even if the storage modulus of PLA-BS tended to increase with the frequency, cyclic tests were not possible at 20 and 30 Hz due to immediate and spectacular buckling of the specimens (Fig. 8).

Fig. 9 allows comparing dynamic properties of PLA-PMMA-BS and reference ABS-PC. At 20 °C and 40 °C, PLA-PMMA-BS showed at least similar, sometimes higher, storage modulus than ABS-PC, whatever the load frequency. At 50 °C, storage modulus of PLA-PMMA-BS dropped of about 200–400 MPa, depending on frequency, while storage modulus of ABS-PC was much less affected (decrease of only about 50 MPa). However, as highlighted before, storage modulus of PLA-PMMA-BS remained at a satisfactory level and the gap to ABS-PC tended to decrease when increasing load frequency (due to "time-temperature equivalence" principle), which is a favorable trend for use in technical parts subjected to high-strain-rate loadings. As underlined before, dynamic properties of PLA-PMMA-BS at 60 °C were prohibitive for use in highly-loaded parts. As expected, storage modulus of ABS-PC remained at a high level, although a drop of about 200 MPa was noticed between 50 °C and 60 °C.

### 3.3. Overview of mechanical performance of PLA-PMMA-BS compared to ABS-PC

Previous Part 1 [7] and present Part 2 of this study provide information about mechanical properties of composition PLA-PMMA-BS over a wide range of strain rate and under a temperature up to 50 °C. For the reasons explained before, a commercial ABS-PC blend was selected as a basis of comparison to assess the

**Table 5**
Glass transition temperature and crystallinity ratio of selected specimens of PLA-based compositions.

| | PLA-PMMA-BS | | PLA-BS | |
|---|---|---|---|---|
| | Sample with weakest tensile properties at 50 °C | Sample with highest tensile properties at 50 °C | Sample with weakest tensile properties at 50 °C | Sample with highest tensile properties at 50 °C |
| $T_g$ (°C) | 66 | 71 | 63 | 64 |
| $X_c$ (%) | 18 | 20 | 15 | 18 |

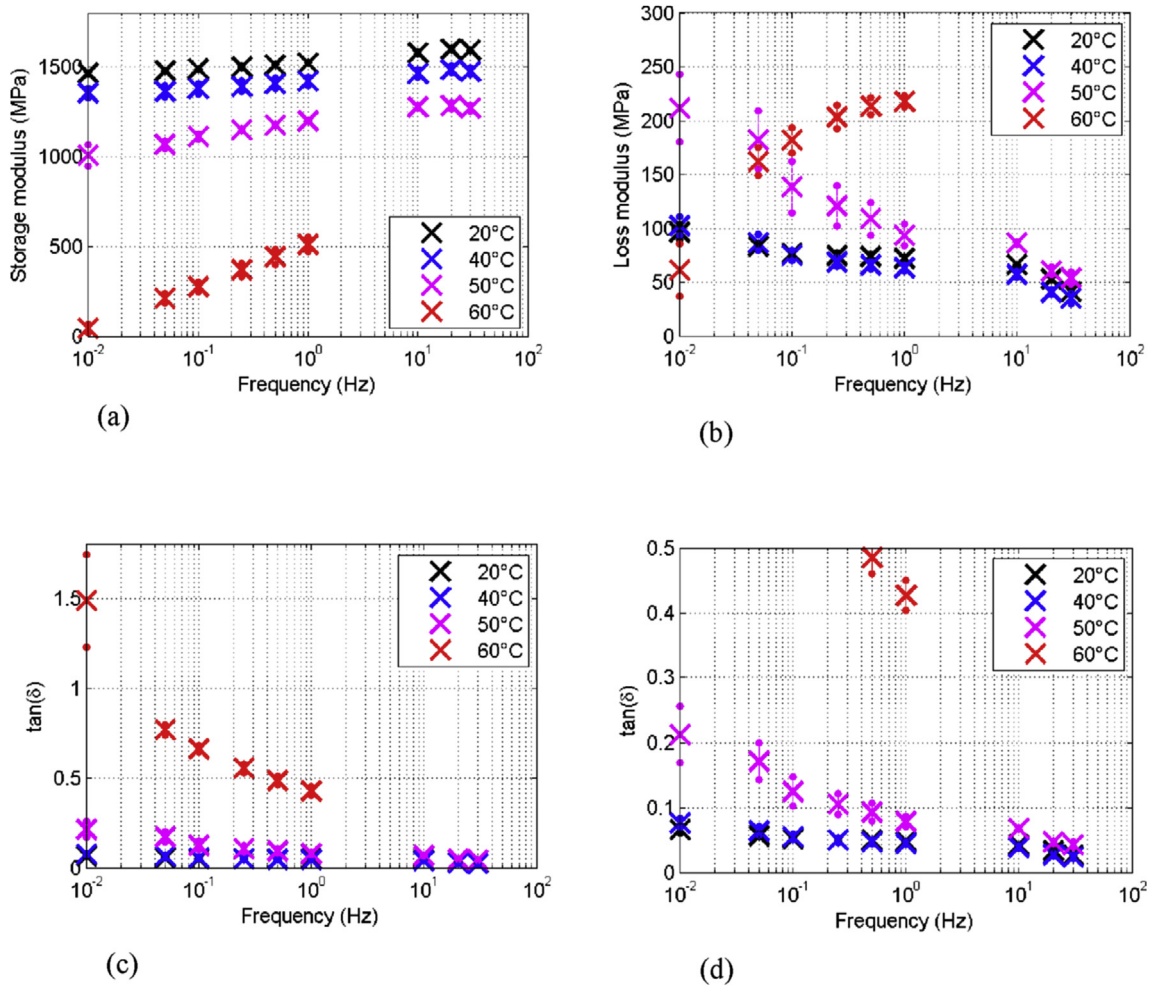


**Fig. 6.** Dynamic properties of PLA-PMMA-BS composition upon load frequency and temperature (Crosses stand for average values, vertical lines delimited by points indicate standard deviation). (a) Storage modulus. (b) Loss modulus. (c) Loss factor. (d) Loss factor: focus on lower values

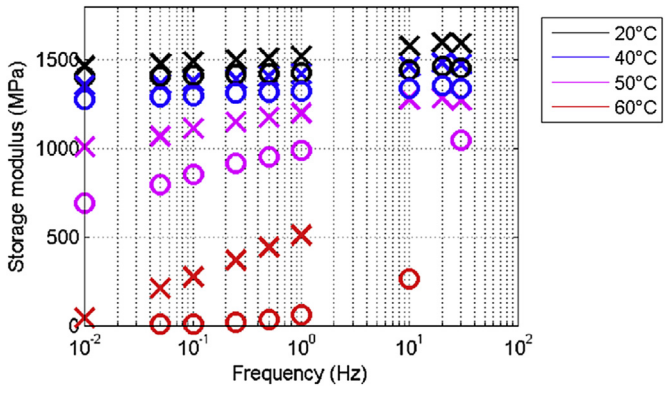


**Fig. 7.** Comparison of dynamic properties of PLA-PMMA-BS and PLA-BS at different load frequency and temperature (crosses: PLA-PMMA-BS, circles: PLA-BS; markers stand for average values; for clarity, standard deviations are not indicated).

potential of PLA-based composition for use in highly loaded technical parts, for instance in the automotive sector. Fig. 10 gives an overview of the mechanical performance of PLA-PMMA-BS compared to ABS-PC. In that Figure, the ratio of the average value of a given property (among elastic modulus, tensile strength, tensile strain at break and tensile volume energy of deformation) of PLA-PMMA-BS divided by that of ABS-PC is plotted for 3 examples of loading conditions, namely quasi-static loading ($\dot{\varepsilon} = 510^{-4}s^{-1}$) at ambient temperature, dynamic loading ($\dot{\varepsilon} = 50s^{-1}$)at ambient temperature and quasi-static loading ($\dot{\varepsilon} = 510^{-3}s^{-1}$) at 50 °C. At ambient temperature, elastic modulus, strain at break and volume energy of deformation of PLA-PMMA-BS are always higher than ABS-PC, whatever the strain rate (*i.e.* from $\dot{\varepsilon} = 510^{-4}s^{-1}$ to 50 $s^{-1}$), while tensile strength is slightly lower (ratio of 0.81–0.91). At 50 °C, the elastic modulus and the tensile strength of PLA-PMMA-BS are about 0.64 and 0.53 times that of ABS-PC but the strain at break and the volume energy of deformation are considerably higher (at least 180 and 10 times higher, respectively). No dynamic tensile tests were performed at 50 °C. However, DMA highlighted the "time-temperature equivalence" principle of PLA-PMMA-BS mechanical behavior. Therefore, it can reasonably be expected that rigidity and strength of PLA-based composition will be higher during dynamic tests at 50 °C than during quasi-static tests at 50 °C. This is undoubtedly a positive trend if aiming at designing material for technical parts subjected to high strain-rate loadings and high temperature.

## 4. Conclusions and future work

Present work is continuation of the study initiated by Bouzouita et al. [6] and pursued by Notta-Cuvier et al. [7] aiming at designing

**Fig. 8.** Buckling of PLA-BS specimen during cyclic loading at 20 Hz and 60 °C.

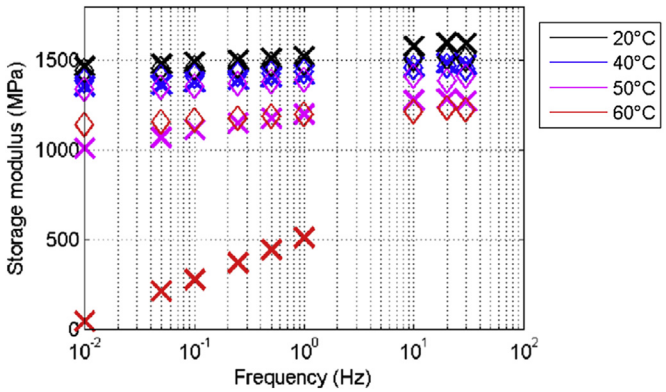


**Fig. 9.** Comparison of dynamic properties of PLA-PMMA-BS and ABS/PC at different load frequency and temperature (crosses: PLA-PMMA-BS, diamonds: ABS-PC; markers stand for average values; for clarity, standard deviations are not indicated).

a toughened PLA-based composition for application in technical parts subjected to severe loading conditions, *i.e.* at high strain rate and/or high temperature.

The optimal composition, *i.e.*58 wt% polylactide (PLA) - 25 wt% poly (methyl methacrylate) (PMMA) - 17 wt% Impact modifier (Biostrong) was selected by Bouzouita et al. [6], as the one that showed the best balance of thermo-mechanical properties in comparison with an ABS-PC blend, as a challenging target for use in automotive applications. Then, it has been demonstrated [7] that PLA-PMMA-BS composition has very appealing mechanical properties, even if it is processed using industrial facilities and output rate compatible with requirements of the automotive sector. In particular, tensile behavior of PLA-PMMA-BS composition was proven to be undoubtedly competitive with that of ABS-PC under a wide range of strain-rate (up to 50 $s^{-1}$), at ambient temperature.

In Part 2 of the study, it has been demonstrated that PLA-PMMA-BS composition also presents interesting mechanical properties

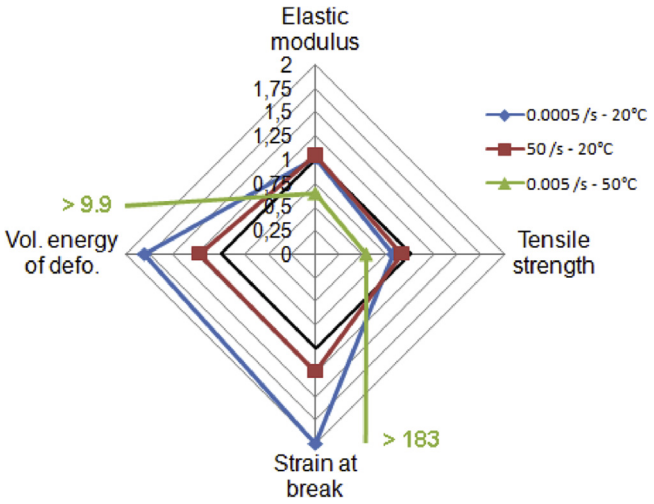


**Fig. 10.** Mechanical performance of PLA-PMMA-BS composition in comparison to reference ABS-PC blend.

when being tested at 50 °C (quasi-static strain rate of 5 $10^{-3}$ $s^{-1}$). Undoubtedly, the addition of PMMA has positive influence on mechanical behavior under higher temperature, even if the gain in glass transition temperature, $T_g$, is low, as evidenced by comparison with behavior of PLA-BS blend. Actually, elastic modulus and tensile strength of PLA-PMMA-BS are 0.6 and 0.5 times those of ABS-PC, respectively, but volume energy of deformation is at least 10 times higher. It is also worth noting that tensile properties of PLA-PMMA-BS at 50 °C are, for instance, of the same order of magnitude than those of a 20 wt% mineral-filled polypropylene frequently used in automotive sector, as evaluated at ambient temperature in previous work [5].

Dynamic Mechanical Analyses revealed that the gap between the storage modulus of PLA-PMMA-BS and ABS-PC tends to decrease at high temperature (up to 60 °C) when increasing loading rate, thus highlighting the "time-temperature equivalence" principle for polymer mechanical behavior. Therefore, it is likely that mechanical performance of PLA-PMMA-BS composition will be suitable for parts subjected to high strain-rate loading under moderately high temperature (to be verified soon based on dynamic tensile tests at high temperature).

Part 1 and 2 of this study demonstrated, therefore, the suitability of PLA-PMMA-BS composition for use in highly loaded technical parts under moderately high temperature. However, due to relatively low $T_g$ (about 60 °C), this composition cannot be reasonably used today for parts submitted to temperature higher than 50 °C (in dashboards, *e.g.*). Further developments are needed to improve thermal properties of that composition. Strategies are currently being explored, such as stereo-complexation of PLLA-PDLA, use of nucleating agents, etc. Incorporation of vegetal fibers may also be an interesting challenge, because it generally leads to a spectacular increase of HDT. In the longer term, aging of PLA-based composition is also a crucial issue, especially because of risk of hydrolysis of PLA matrix, and deserves further work.

## Acknowledgments

The authors would like to sincerely thank Reydel Automotive France, and in particular Mr Goislard, Mr Germain and Mr Pouille, for having made their injection molding facilities available to us. LAMIH authors are grateful to CISIT, the Nord-Pas-de-Calais Region, the European Community, the Regional Delegation for Research

and Technology, the Ministry of Higher Education and Research and the National Center for Scientific Research for their financial support. UMONS authors are grateful to the Region Wallonne and European Community (FEDER, FSE) in the frame of Pole d'Excellence Materia Nova INTERREG IV-NANOLAC project and in the excellence programOPTI$^2$MAT for their financial support. CIRMAP thanks the Belgian Federal Government Office Policy of Science (SSTC) for general support in the frame of the PAI-7/05. J.-M. Raquez is Chercheur qualifie by the F.R.S.-FNRS (Belgium).

## References

[1] E.T.H. Vink, K.R. Rabago, D.A. Glassner, P.R. Gruber, Applications of life cycle assessment to NatureWorksTM polylactide (PLA), Polym. Degrad. Stab. 80 (3) (2003) 403.
[2] R. Auras, L.-T. Lim, S.E.M. Selke, H. Tsuji, Poly (Lactic Acid): Synthesis, Structures, Properties, Processing, and Applications, John Wiley & Sons, Hoboken, NH, USA, 2010.
[3] L.-T. Lim, R. Auras, M. Rubino, Processing technologies for poly(lactic acid), Prog. Polym. Sci. 33 (8) (2008) 820.
[4] D. Notta-Cuvier, J. Odent, R. Delille, M. Murariu, F. Lauro, J.M. Raquez, B. Bennani, P. Dubois, Tailoring polylactide (PLA) properties for automotive applications: effect of addition of designed additives on main mechanical properties, Polym. Test. 36 (2014) 1.
[5] D. Notta-Cuvier, M. Murariu, J. Odent, R. Delille, A. Bouzouita, J.M. Raquez, F. Lauro, P. Dubois, Tailoring polylactide properties for automotive applications: effects of co-addition of halloysite nanotubes and selected plasticizer, Macromol. Mater. Eng. 300 (2015) 684.
[6] A. Bouzouita, C. Samuel, D. Notta-Cuvier, J. Odent, F. Lauro, P. Dubois, J.-M. Raquez, Design of highly tough poly(L-lactide)-based ternary blends for automotive applications, J. Appl. Polym. Sci. 133 (19) (2016). http://dx.doi.org/10.1002/APP.43402.
[7] D. Notta-Cuvier, A. Bouzouita, R. Delille, G. Haugou, J.-M. Raquez, F. Lauro, P. Dubois, Design of toughened PLA based material for application in structures subjected to severe loading conditions. Part 1. Quasi-static and dynamic tensile tests at ambient temperature, Polym. Test. 54 (2016) 233.
[8] CorbionPurac. PLA bioplastics: A driving force in automotive. CorbionPurac. http://www.corbion.com/bioplastics/pla-markets/automotive. Accessed October 4th 2016.
[9] Teijin & Kansai University. Teijin & Kansai University develop new piezoelectric material, http://www.teijin.com/news/2012/ebd120906.pdf, Accessed October 4th 2016.
[10] K.S. Anderson, K.M. Schreck, M.A. Hillmyer, Toughening polylactide, Polym. Rev. 48 (2008) 85.
[11] M. Murariu, A. Da Silva Ferreira, M. Alexandre, P. Dubois, Polylactide (PLA) designed with desired end-use properties: 1. PLA compositions with low molecular weight ester-like plasticizers and related performances, Polym. Adv. Technol. 19 (2008) 636.
[12] J. Odent, Y. Habibi, J.-M. Raquez, P. Dubois, Ultra-tough polylactide-based materials synergistically designed in the presence of rubbery ε-caprolactone-based copolyester and silica nanoparticles, Comp. Sci. Tech. 84 (2013) 86.
[13] J.-M. Raquez, Y. Habibi, M. Murariu, P. Dubois, Polylactide (PLA)-based nanocomposites, Prog. Polym. Sci. 38 (2013) 1504.
[14] S. Sinha Ray, K. Yamada, M. Okamoto, K. Ueda, Polylactide-layered silicate nanocomposite: a novel biodegradable material, Nano Lett. 2 (2002) 1093.
[15] M. Murariu, A. Doumbia, L. Bonnaud, A.L. Dechief, Y. Paint, M. Ferreira, C. Campagne, E. Devaux, P. Dubois, High-performance polylactide/ZnO nanocomposites designed for films and fibres with special end-use properties, Biomacromolecules 12 (5) (2011) 1762.
[16] M. Jamshidian, E.A. Tehrany, M. Imran, M. Jacquot, S. Desobry, Poly-lactic acid: production, application, nanocomposite, and release studies, Compr. Rev. Food Sci. Food Saf. 9 (2010) 552.
[17] J.L. Eguiburu, J.J. Iruin, M.J. Fernandez-Berridi, J. San Roman, Blends of amorphous and crystalline polylactides with poly(methyl methacrylate) and poly(methyl acrylate): a miscibility study, Polymer 39 (1998) 6891.
[18] G. Zhang, J. Zhang, S. Wang, D. Shen, Miscibility and phase structure of binary blends of polylactide and poly(methyl methacrylate), J. Polym. Sci. Part B Polym. Phys. 41 (2003) 23.
[19] S.H. Li, E.M. Woo, Immiscibility-miscibility phase transitions in blends of poly(L-lactide) with poly(methyl methacrylate), Polym. Int. 57 (2008) 1242.
[20] C. Samuel, J.M. Raquez, P. Dubois, PLLA/PMMA blends: a shear induced miscibility with tunable morphologies and properties? Polymer 54 (15) (2013) 3931.
[21] J.R. Dorgan, J. Janzen, D.M. Knauss, S.B. Hait, B.R. Limoges, M.H. Hutchinson, Fundamental solution and single-chain properties of polylactides, J. Polym. Sci. Part B Polym. Phys. 43 (2005) 3100.
[22] M.A. Sutton, J.-J. Orteu, H.W. Schreier, Image correlation for shape, motion and deformation measurements. Basic concepts, Theory and Applications, Springer Edition, New York, 2009.
[23] J. Rieger, The glass transition temperature $T_g$ of polymers - comparison of the values from differential thermal analysis (DTA, DSC) and dynamic mechanical measurements (torsion pendulum), Polym. Test. 20 (2001) 199.
[24] T. Sterzyński, J. Tomaszewska, J. Andrzejewski, K. Skórczewska, Evaluation of glass transition temperature of PVC/POSS nanocomposites, Compos. Sci. Technol. 117 (2015) 398.